TECHNICAL NOTES AND RESEARCH BRIEFS

Paul B. Ostergaard
10 Glenwood Way, West Caldwell, NJ 07006

Editor's Note: Original contributions to the Technical Notes and Research Briefs section are always welcome. Manuscripts should be double-spaced, and ordinarily not longer than about 1500 words. There are no publication charges, and consequently, no free reprints; however, reprints may be purchased at the usual prices.

Implementation details of a computation model of the inner hair-cell/auditory-nerve synapse

[43.64.Bt, 43.64.Pg, 43.64.Nf]

Ray Meddis, Michael J. Hewitt, and Trevor M. Shackleton

Department of Human Sciences, University of Technology, Loughborough, Leicestershire LE11 3TU, England

INTRODUCTION

A simple and computationally efficient model of auditory-neural transduction at the inner hair cell has recently been described, (Meddis, 1986a and 1988). This paper briefly presents a short computer program to implement the model, an exploration of the effects of modifying the parameters of the model, a new set of parameters for simulating an auditory nerve fiber showing a medium rate of spontaneous activity with extended dynamic range, and some methods of quickly estimating some of the characteristics. It is intended as advice for researchers who wish to implement the model as part of a speech recognition device or as input to another model of more centrally located neurophysiological functions.

I. THE MODEL

The input to the model is the pattern of vibration at a particular point along the cochlear partition and its output is an excitation function representing the fluctuating instantaneous probability of a spike event in a post-synaptic auditory nerve fiber. The model assumes that three reservoirs of transmitter substance exist within the hair cell and that the rate of transmitter release from the cell into the pre-synaptic cleft is a function of the instantaneous displacement of the neighboring cochlear partition. The physical basis of the model is undoubtedly controversial but, in operation, the model provides a fast and useful simulation of many important features of auditory nerve activity. It generates realistic post-stimulus time histograms for silence and pulsed pure tones and shows rapid and short-term adaptation. Phase locking to repetitive stimuli also occurs for low-frequency stimuli but is restricted, naturalistically, at higher frequencies. A particular feature of the model is its suitability for use with arbitrary stimuli such as speech and noise signals.

A full description of the model and its ability to match empirical results are given elsewhere (Meddis, 1986a, 1988). It is illustrated in Fig. 1 and works as follows. A quantity $q(t)$ of packets of transmitter substance is held in a free transmitter pool that lies close to the cell membrane. These packets are released across the membrane into the cleft at a rate determined by the instantaneous degree of displacement of the basilar membrane $S(t)$. The release fraction $k(t)$ is computed using Eq. (4) in Fig. 1. The total amount of transmitter in the cleft $c(t)$ determines the instantaneous post-synaptic probability of spike occurrence. The release fraction $k(t)$ is intended to reflect the permeability of the membrane at the synapse. It is given as a direct function of stimulus intensity, $s(t)$, and therefore avoids speculation as to how the effect is mediated. The actual probability can be found by multiplying by a constant h.

Transmitter in the cleft is continuously subject to depletion through dissipation at a rate $lc(t)$ s^{-1}. Transmitter is also recovered from the cleft into the cell at a rate $rc(t)$ s^{-1}. Recovered transmitter, $w(t)$, is held in a reprocessing pool and is released again into the free transmitter pool at a rate $xw(t)$ s^{-1}. The free transmitter pool is also subject to continuous replenishment at a rate $y\{M\text{-}q(t)\}$ s^{-1}. Here, M specifies the maximum number packets of transmitter in the free pool. It can be set arbitrarily to one so that all other quantities are viewed as fractions of this maximum. No analytic solution exists for the equations except for periods of silence. These equations are therefore evaluated iteratively using small time intervals, dt.

The model is rich in parameters and the following comments are in order. We continue to explore improvements and simplifications to the model but this note has adhered strictly to the model published earlier for reasons of consistency. However, three parameters governing the premeability function (g, A, B) is clearly a luxury. They do allow us to experiment with different permeability functions but should eventually reduce to a pair or a single parameter. Similarly, the firing-rate factor h is simply a scale factor and the purpose of the maximum transmitter quantity M is to give the user the choice of working with actual numbers of transmitter packets or, as we prefer, to work in terms of proportions. Once a preference has been declared, these two quantities can be combined into a single parameter.

II. COMPUTER PROGRAM

The short computer program in Fig. 2 is a complete BASIC implementation of the model suitable for use on any desktop micro. In its present form the program can be used to explore the model and become acquainted with its properties prior to incorporation into a final application program.

The sampling rate, dt, can be specified by the user but values greater than 0.1 ms are not advised. With certain sets of parameters, much shorter sampling intervals are required to avoid negative quantities appearing in reservoirs.

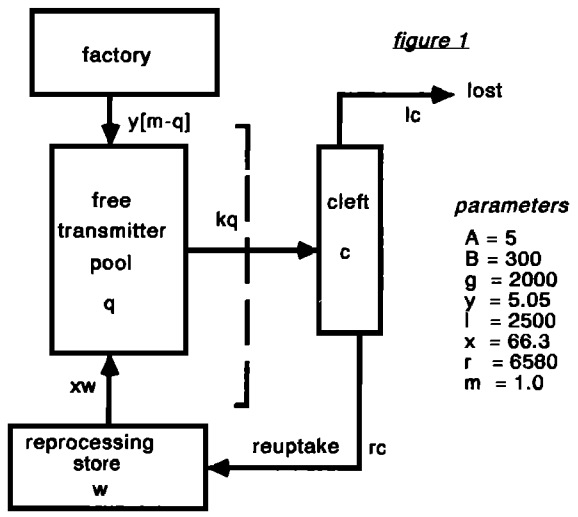

figure 1

(1) $dq/dt = y(m-q(t)) + xw(t) - k(t)q(t)$

(2) $dc/dt = k(t)q(t) - lc(t) - rc(t)$

(3) $dw/dt = rc(t) - xw(t)$

(4) $k(t) = g.dt[s(t)+A]/[s(t)+A+B]$ for $[s(t)+A] > 0$

$k(t) = 0$ for $[s(t)+A] < 0$

FIG. 1. Summary of the operation of the hair cell model with differential equations and parameters for a high spontaneous rate fiber. The instantaneous firing rate of the fiber is a linear function of c (the cleft contents). Here, $S(t)$ is the instantaneous amplitude of the signal. When using real arithmetic, the value of m (maximum transmitter) is conveniently set to 1.

 0001-4966/90/041813-04$00.80

```
 10 dt=0.00005          :REM  Epoch length
 20 :
 30 M=1                 :REM  Maximum free transmitter
 40 A=5                 :REM  Used in permeability equation
 50 B=300               :REM  Used in permeability equation
 60 g=2000              :REM  Used in permeability equation
 70 y=5.05              :REM  Replenishment rate
 80 l=2500              :REM  Rate of loss from the cleft
 90 r=6580              :REM  Rate of return from the cleft
100 x=66.31             :REM  Rate of release from reprocessing to free transmitter
110 h=50000             :REM  Convert cleft contents to firing probability
120 :
130 gdt=g*dt            :REM  Adjust rate using epoch length
140 ydt=y*dt
150 ldt=l*dt
160 rdt=r*dt
170 xdt=x*dt
180 hdt=h*dt
190                     :REM  Set initial reservoir contents at
200                     :REM   spontaneous levels
210 kt=g*A/(A+B)        :REM  kt is membrane permeability
220 q=c*(l+r)/kt        :REM  Free transmitter
230                     :REM  Cleft contents - linked to firing probability
240 c=M*y*kt/(l*kt+y*(l+r))
250 w=c*r/x             :REM  Reprocessing store
260 :
270 :
280 dB=80               :REM  Resettable amplitude of signal
290 amp=10^(dB/20-1.35) :REM  30 dB is rms=1
300 frequency=1000
310 endsilence=.01      :REM  Duration of initial silence
320 lasttime=0          :REM  Time of last spike (for refractory effect)
330 events=0:           :REM  Counts number of spikes so far
340 A$=" "              :REM  Marks the event epoch
350 :
360   :REM  Model runs for 1 second, begins with silence then 1kHz tone
370   :REM  st is a sinusoid but can be any signal
380 :
390 CLS
400 PRINT" time","   kt","    q","   cleft","  spikes","   w","  stimulus"
410 :
420 FOR time = dt TO 1 STEP dt
430                     :REM  Compute stimulus amplitude
440 :
450 IF time>endsilence THEN st=amp*SIN(time*2*PI*frequency) ELSE st=0
460 IF st+A>0 THEN kt=gdt*(st+A)/(st+A+B) ELSE kt=0
470 :
480                     :REM  Compute change quantities
490 IF M >= q THEN replenish=ydt*(M-q)
500 eject=kt*q
510 loss=ldt*c
520 reuptake=rdt*c
530 reprocess=xdt*w
540                     :REM  Now update reservoir quantities
550 q=q+replenish-eject+reprocess
560 c=c+eject-loss-reuptake
570 w=w+reuptake-reprocess
580                     :REM  If not in refractory phase, apply
590                     :REM   stochastic process
600 IF time-lasttime>.001 AND hdt*c>RND(1) THEN events=events+1:
                                                lasttime=time: A$="*"
610 PRINT time,kt,q,c,A$+" ";events,w,"  ";st : A$=" "
620 NEXT
630 STOP
```

FIG. 2. BASIC program for implementing the procedure shown in Fig. 1 and described in the text.

The state of the model is determined by the three quantities representing reservoir contents, q, c, w, which can be set to any initial positive value less than M. In silence, these quantities will rapidly settle to values appropriate to the parameters of the model and independent of the initial values used. The parameters of the model are M, A, B, g, y, l, r, x, and a firing-rate factor h. Some of these parameters need to be adjusted using dt to obtain working values for the equations and to allow a check to be made that none of the release fractions are greater than 1. Thus, M is, roughly speaking, the maximum amount of transmitter in the system. It is normally set to 1 and all values are understood to be fractions of M. For integer implementations, however, M can be set to a value such as 1000 or whatever is believed to be the number of packets of transmitter in the system.

The incidence of spikes is determined by a uniform random number generator subject to two conditions: (a) no spike can follow another within 1 ms (refractory period) and (b) the random number must be smaller than the value corresponding to the cleft contents multiplied by a rate factor. The rate factor h is most conveniently set by noting the cleft contents after a long period of silence and matching this to a desired spontaneous rate of firing:

rate factor = spont rate/cleft contents.

The program illustrates the reponse of the model to a brief (0.01-s) period of silence followed by a longer 80-dB, 1-kHz, sinusoidal toneburst (0.99 s). These values are easily altered. The dB rating is arbitrary but, on this scale, 30 dB corresponds to a signal rms of 1. The program computes all quantities of transmitter moving from one reservoir to another before updating the reservoir content values. All variable quantities are printed out for inspection on each cycle.

III. CHOOSING PARAMETERS

A. Method

No simple way has been found to generate individual parameters that will produce a required set of characteristics of the system; the originally published set of parameters were found largely by trial and error using guided random walks. Table I gives the parameters used in Meddis (1988) along with the consequences of changing individual parameters by 50%. Each set of parameters is evaluated using 250-ms, 1-kHz tone bursts of increasing amplitude from 20 to 120 dB in 5-dB steps interspersed with long silent intervals. Tone bursts had a 2.5-ms rise time. The following output measures are generated for each configuration of parameters:

(i) the spontaneous rate (rate after 500 ms using a -20-dB stimulus);

(ii) the saturated rate (rate after 250 ms using a 120-dB stimulus);

(iii) the rate-intensity threshold (lowest level to show a 5% increase in event rate above spontaneous rate);

(iv) the saturation threshold (lowest level to show a rate within 5% of the saturated rate);

(v) rapid and short-term adaptation time constants of the rate response to stimuli 20 and 50 dB above rate-intensity threshold (see Meddis, 1986b and 1988 for methods for computing these);

(vi) recovery time constant after 120-dB stimulus offset;

(vii) Rose *et al.*'s (1967) phase-locking synchronization measure at 1 kHz and at 5 kHz (50% signifies no effective phase locking).

B. Results

The effect of changing individual parameters in a nonlinear system depends on the initial configuration. However, for modelers starting from this set of parameters, some useful points do emerge.

(1) Increasing A (a permeability constant) raises the spontaneous rate and both the rate threshold and the saturation rate threshold. It also speeds adaptation to low amplitude stimuli.

(2) Increasing B (a permeability constant) increases the dynamic range of the fiber from 25 to 35 dB and depresses the spontaneous rate. It also speeds rapid adaptation to low-amplitude stimuli.

(3) Reducing g (release rate) lowers the spontaneous rate and increases dynamic range. It slows adaptation to high-amplitude stimuli.

(4) Reducing y (replenishment rate) lowers spontaneous and saturated firing rates.

(5) Reducing l (cleft loss rate) raises firing rates, increases the dynamic range, slows adaptation to all stimuli, and reduces phase locking.

(6) Reducing r (recovery rate) increases spontaneous firing rate and selectively speeds short-term adaptation but, more importantly, is the only parameter that substantially reduces phase locking.

(7) Reducing x (reprocessing rate) slows short term and speeds rapid adaptation to low-amplitude stimuli.

IV. SIMULATING MEDIUM SPONTANEOUS-RATE FIBERS

The spontaneous rates of discharge of populations of auditory nerve fibers occur in a bimodal distribution (Kiang *et al.*, 1965) and possibly a trimodal distribution (Liberman, 1978). The fiber simulated in Table I would be characterized as a "high" spontaneous-rate fiber. Fibers with a substantially lower rate of discharge typically show a much wider dynamic range and modelers may wish to include such fibers in their simulations. Geisler *et al.* (1985) have shown, using statistically defined criteria, that fibers with medium rates of spontaneous discharge have only slightly raised rate thresholds and that earlier contrary views may be based upon less adequate criteria.

The spontaneous rate of discharge has been reduced by changing the permeability parameters A, B, and g, as shown in Table II. These changes result in a spontaneous discharge rate of only 15 events per second, a slightly raised rate threshold (+ 5 dB) and a greatly increased dynamic range (50–95 dB). This medium spontaneous-rate unit shows slower rates of adaptation, a result that is consistent with the findings of Rhode and Smith (1985).

Our model offers an explanation of the difference between the two types of fibers in terms of the permeability characteristics of the inner hair cell innervating the fiber. The lower permeability of the cell causes lower rates of spontaneous firing, a less vigorous response to stimulus onset, and slower depletion of available transmitter. It does not affect the steady-state response rate after adaptation because this is mainly dependent upon a balance between the rate of loss of transmitter from the system (l) and the rate of replenishment (y), as shown in Table I.

Geisler (1981) has modeled the difference between the two types of fibers in terms of the reduced sensitivity of the post-synaptic membrane for

TABLE I. The effects of changing a single model parameter on various measures of single fiber response to 250-ms 1-kHz tone bursts (see text). All parameter values are reduced except A and B that are increased to show their effect upon dynamic range more clearly. Asterisks indicate a change greater than 10% from baseline. Fixed parameters were $M = 1$, $h = 50\,000$, and $dt = 0.05$ ms.

	Meddis (1988)	*A*	*B*	*g*	*y*	*l*	*r*	*x*
Parameter								
A	5	10						
B	300		600					
g release	2000			1000				
Y replenish	5.05				2.5			
l loss from cleft	2500					1250		
r recovery	6580						3270	
x reprocessing	66.31							33
Spontaneous rate	64	78*	47*	47*	39*	102*	74*	64
Saturated rate	99	99	99	97	49*	198	99	100
rate-threshold (dB SL)	45	50*	45	45	45	45	45	45
sat-threshold (dB SL)	70	75	80*	80*	70	80*	65	75
Adaptation time constants (ms)								
T2 (+ 20 dB) short term	75	61*	72	78	82	97*	51*	99*
T2 (+ 50 dB) short term	57	56	57	72*	57	89*	36*	98
T1 (+ 20 dB) rapid	7.7	3.2*	6.8*	7.2	7.8	4.5*	8.1	5.4*
T1 (+ 50 dB) rapid	1.2	1.3	1.3	2.2*	1.2	1.1	1.2	1.2
synchronization(1 kHz)%	91	91	91	91	91	87	83*	91
synchronization(5 kHz)%	62	62	63	63	63	61	58*	63

low spontaneous rate fibers. We have not explored this possibility, but it is unlikely that post-synaptic sensitivity changes can predict adaptation rate differences such as those observed by Rhode and Smith (1985).

TABLE II. Effect of changing all permeability parameters to produce a medium spontaneous -rate fiber with higher threshold and wider dynamic range. Asterisks indicate changed parameters. Fixed parameters were $M = 1$, $h = 50\,000$, $dt = 0.05$ ms.

	Meddis (1988)	Medium spontaneous rate fiber
Parameter		
A	5	10*
B	300	3000*
g release	2000	1000*
y replenish	5.05	5.05
l loss	2580	2500
r recovery	6580	6580
x reprocessing	66.31	66.31
Spontaneous rate	64	15
Saturated rate	99	97
Rate threshold (dB SL)	45	50
Sat threshold (dB SL)	70	95
Adaptation time constants (ms)		
*T*2 (+ 20 dB) short term	75	99
*T*2 (+ 50 dB) short term	57	61
*T*1 (+ 20 dB) rapid	7.7	11.1
*T*1 (+ 50 dB) rapid	1.2	3.2
synchronization (1 kHz)%	91	91
synchronization (5 kHz)%	62	63

V. QUICK CALCULATION OF SYSTEM CHARACTERISTICS

For a given set of parameters, some characteristics of the system can be directly specified. It is an incomplete list but may be useful for some purposes. For example, it is useful to know the values of reservoir contents during spontaneous firing. This allows us to set up the model before introducing a stimulus in a manner consistent with a long preceding silence.

Using analytical approximations it is possible for a given set of parameters to determine the spontaneous and saturated firing rates as well as the rate-intensity and saturation thresholds.

The spontaneous firing rate is determined from the equilibrium state of the system with no input. That is, the reservoir contents do not change in time so Eqs. (1)–(3) of Fig. 1 can be rewritten with the derivatives set to zero. Upon solving the three simultaneous equations we obtain

$$c = k\,ym/[y(l + r) + kl],$$

$$q = c\,(l + r)/k,$$

$$w = c\,r/x,$$

where

$$k = gA/(A + B).$$

These equations are exact, the spontaneous firing rate is obtained in the usual way from c.

We may obtain an approximation for the saturated firing rate by considering the behavior of the system at a frequency sufficiently high for phase locking not to occur. In this case, once the nerve has adapted, the contents of the reservoirs do not vary in time. We may therefore use the above equation for the cleft contents, c, but with a modified value of the permeability function k. For the range of parameters considered in this paper, at saturation

$$kl \gg y(l + r)$$

so the cleft contents are given approximately by

$$c \approx ym/l.$$

To determine the rate-intensity and saturation thresholds we again use the equation for cleft contents, but with the permeability function k replaced by $\langle k \rangle$, the average of k over a single cycle of input.

There is no simple analytical solution for the average of $k(t)$ over a

single cycle, but it is a simple matter to numerically integrate to obtain $\langle k \rangle$ and then use this in the equation for cleft contents. The rate-intensity and saturation thresholds may then be obtained by interpolating between the calculated values of cleft contents at different stimulus levels.

Although these approximations are formally derived as a high-frequency limiting case, simulations show that these results are valid over the entire frequency range.

ACKNOWLEDGMENTS

We would like to thank Roy Patterson, Strange Ross, Peter Assman, and Quentin Summerfield for useful discussions and helpful suggestions. The work is supported by an SERC grant.

Geisler, C. D. (**1981**). "A model for discharge patterns of primary auditory-nerve fibers," Brain Res. **212**, 198–201.

Geisler, C. D., Deng, L., and Greenberg, S. R. (**1985**). "Thresholds for primary auditory fibers using statistically defined criteria," J. Acoust. Soc. Am. **77**, 1102–1109.

Kiang, N. Y. S, Watanabe, T., Thomas, E. C., and Clark, L. F. (**1965**). *Discharge Patterns of Single Fibers in the Cat's Auditory Nerve* (MIT, Cambridge, MA).

Liberman, M. C. (**1978**). "Auditory-nerve response from cats raised in a low-noise chamber," J. Acoust. Soc. Am. **63**, 442–455.

Meddis, R. (**1986a**). "Simulation of mechanical to neural transduction in the auditory receptor," J. Acoust. Soc. Am. **79**, 702–711.

Meddis, R. (**1986b**). "Comments on 'Very rapid adaptation in the guinea pig auditory nerve' by Yates, G. K. *et al.*, 1985," Hear. Res. **23**, 287–290.

Meddis, R. (**1988**). "Simulation of auditory-neural transduction: Further studies," J. Acoust. Soc. Am. **83**, 1056–1063.

Rhode, W. S., and Smith, P. H. (**1985**). "Characteristics of tone-pip response patterns in relationship to spontaneous rate in cat auditory nerve fibers," Hear. Res. **18**, 159–168.

Rose, J. E., Brugge, J. F., Anderson, D. J., and Hind, J. E. (**1967**). "Phase-locked response to low-frequency tones in single auditory nerve Fibers of the squirrel monkey," J. Neurophysiol. **30**, 767–793.

Quality evaluation by acousto-ultrasonic testing of composites [43.35.Cg, 43.40.Le]

A report prepared by Alex Vary of Lewis Research Center reviews acousto-ultrasonic technology for nondestructive testing. The report discusses principles, suggests advanced signal-analysis schemes for development, and presents potential applications.

Acousto-ultrasonics has been applied principally to assess defects in laminated and filament-wound fiber-reinforced composite materials. The technique can be used to determine variations in such properties as tensile, shear, and flexural strengths and reductions in strength and toughness caused by defects. It can be used to evaluate states of cure, porosities, orientation of fibers, volume fractions of fibers and matrices, and qualities of interlaminar bonds.

The term "acousto-ultrasonics" is a contraction for "acoustic-emission simulation with ultrasonic sources." Conventional acoustic-emission testing depends on loading a part to excite spontaneous stress waves like those that accompany plastic deformations and the growth of cracks. Acousto-ultrasonics differs mainly in that the ultrasonic waves are benign and are generated externally by pulsed sources (usually piezotranducers).

In a typical apparatus, a transmitting probe and a receiving probe are placed a specified distance apart on the same side of the part under test. The sending-and-receiving pair can be moved about as a unit to scan the part. Signal-processing instrumentation analyzes the received sound to generate a map of variations in the properties of the material.

The sensitivity of the acousto-ultrasonics has already been demonstrated experimentally. The technology has been used to detect and quantify subtle but significant variations in strength and resistance to fracture of fiber-reinforced composites. This achievement is remarkable because it was accomplished with relatively unsophisticated signal-processing and signal-analysis procedures.

Although acousto-ultrasonic technology has been used on polymer-matrix composites, it is applicable to such other composite materials as metals reinforced by fibers and ceramic-matrix composites. The use of acousto-ultrasonics should be considered whenever it is necessary to quantify damage or degradation of properties after composites have been exposed to hostile environments.

Further information is contained in NASA Report TM-89843 [N87-20562], "The Acousto-Ultrasonic Approach" available from NTIS, Springfield, VA 22161.

Optical measurement of sound pressure [43.35.Sx, 43.25.Zx]

An optical technique that can be used to measure acoustic pressure without direct contact has been developed by Eugene H. Trinh, Mark Gaspar, and Emily W. Leung of CalTech for NASA's Jet Propulsion Laboratory. The technique is especially valuable where it is necessary to measure in a remote, inaccessible, or hostile environment or to avoid perturbation of the measured region. In the original application, the technique was used to measure the acoustic pressure around a sphere acoustically levitated in a furnace. Because the measurements are almost instantaneous, a possible application of the technique is to generate feedback control signals for acoustic levitators.

A laser beam is directed at the region of high acoustic pressure to be measured. The sound causes rapid alterations of density and, therefore, of the index of refraction, and the alternations in turn produce oscillatory deflections of the beam. The deflection is proportional to the acoustic pressure. The laser beam has a negligible influence on the acoustic field.

After passing through the region of interest, the beam is focused onto a knife edge, as in a schlieren system as shown in Fig. 1. The knife edge is adjusted to intercept all or part of the undeflected beam so that the portion that passes the edge and falls on a photodetector varies with the deflection. Thus the greater the acoustic pressure and the deflection of the beam, the greater the intensity of the deflected beam and the amplitude of the output of the photodetector. A detailed map of the pressure field can be obtained by scanning the field in three orthogonal directions. More information can be obtained from Manager, Technology Transfer Division, P. O. Box 8757, Baltimore/Washington International Airport, MD 21240.

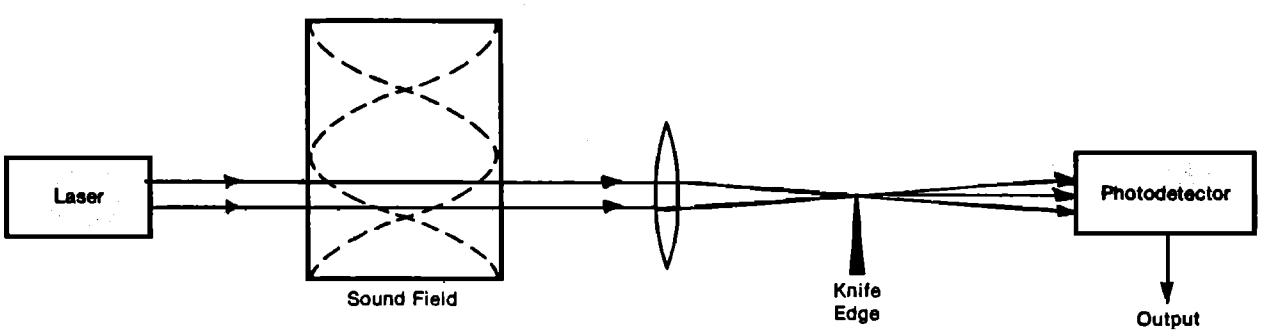

FIG. 1. The sound field deflects the laser beam proportionally to its amplitude. A knife edge intercepts the undeflected beam, allowing only the deflected beam to reach a photodetector. The apparatus is calibrated by comparing the output of the photodetector with that of a microphone.